# High Methane Storage Capacity in Aluminum Metal−Organic Frameworks

Felipe Gándara, Hiroyasu Furukawa, Seungkyu Lee, and Omar M. Yaghi*

Department of Chemistry, University of California−Berkeley, Materials Sciences Division, Lawrence Berkeley National Laboratory, and Kavli Energy NanoSciences Institute at Berkeley, University of California−Berkeley, Berkeley, California 94720, United States

Ⓢ *Supporting Information*

**ABSTRACT:** The use of porous materials to store natural gas in vehicles requires large amounts of methane per unit of volume. Here we report the synthesis, crystal structure and methane adsorption properties of two new aluminum metal−organic frameworks, MOF-519 and MOF-520. Both materials exhibit permanent porosity and high methane volumetric storage capacity: MOF-519 has a volumetric capacity of 200 and 279 $cm^3$ $cm^{-3}$ at 298 K and 35 and 80 bar, respectively, and MOF-520 has a volumetric capacity of 162 and 231 $cm^3$ $cm^{-3}$ under the same conditions. Furthermore, MOF-519 exhibits an exceptional working capacity, being able to deliver a large amount of methane at pressures between 5 and 35 bar, 151 $cm^3$ $cm^{-3}$, and between 5 and 80 bar, 230 $cm^3$ $cm^{-3}$.

Methane is the main component of natural gas and represents about two-thirds of the fossil fuels on earth, yet it remains the least utilized fuel. Currently there is a great interest in expanding the use of methane for fueling automobiles because of its wide availability and its lower carbon emission compared to petroleum. A current challenge for the implementation of this technology is to find materials that are able to store and deliver large amounts of methane near room temperature and at low pressures. The U.S. Department of Energy (DOE) has initiated a research program aimed at operating methane storage fueling systems at room temperature and desirable pressures of 35 and 80 bar, and as high as 250 bar, pressures relevant to commercially and widely available equipment.[1] Metal−organic frameworks (MOFs)[2] are known to be useful in the storage of gases,[3] including methane.[4] Among the many MOFs studied for methane storage are HKUST-1,[5,6] Ni-MOF-74,[6,7] MOF-5,[8,9] MOF-177,[9,10] MOF-205,[9] MOF-210,[9] and PCN-14,[6,11] which stand out as having some of the highest total volumetric storage capacities. Since the automobile industry requires that 5 bar of methane pressure remains unused in the fuel tank, a parameter termed working capacity (illustrated in Scheme 1) is the key to evaluating the performance of methane storage materials. At present, the highest working capacities reported for a MOF are 153 and 200 $cm^3$ $cm^{-3}$, respectively, at 35 and 80 bar for the copper(II)-based MOF HKUST-1. Extensive work is ongoing to find materials whose working capacity is higher than that found for this material.

Here, we report the synthesis, X-ray single crystal structure, porosity, and methane adsorption properties for two aluminum

**Scheme 1**[a]
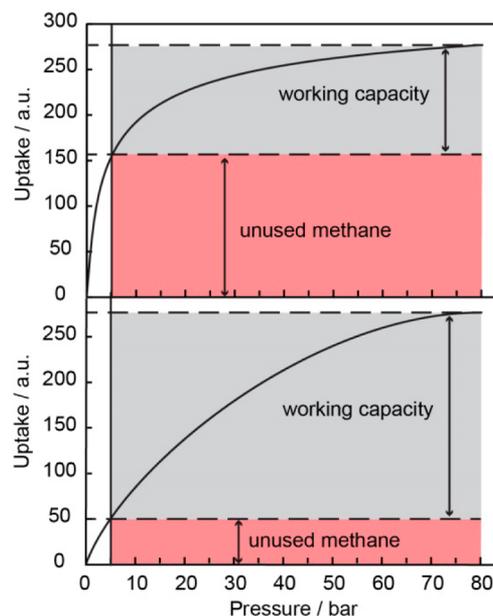


[a]Working capacity is defined as the usable amount of methane that results from subtracting the uptake at the operational desorption pressure (5 bar) from the uptake at the maximum adsorption operational pressure. For materials with large total uptake, the working capacity might be substantially reduced if a large amount of methane cannot be desorbed at the operational desorption pressure remaining unutilized in the fuel tank.

based MOFs [termed MOF-519: $Al_8(OH)_8(BTB)_4(H_2BTB)_4$, and MOF-520: $Al_8(OH)_8(BTB)_4(HCOO)_4$, BTB = 4,4′,4″-benzene-1,3,5-tryil-tribenzoate], one of which (MOF-519) has working capacities of 151 and 230 $cm^3$ $cm^{-3}$, respectively, at 35 and 80 bar, with the first rivaling that of HKUST-1 and the second exceeding the values obtained for all the top performing MOFs under these conditions.

Microcrystalline powder of MOF-519 was used to measure the methane uptake capacity. The sample was prepared by heating a mixture containing aluminum nitrate, $H_3BTB$, nitric acid, and *N,N*-dimethylformamide (DMF) at 150 °C for 4 days.[12] A modified synthesis with higher concentration of nitric acid resulted in lower yield but afforded a single crystal, which
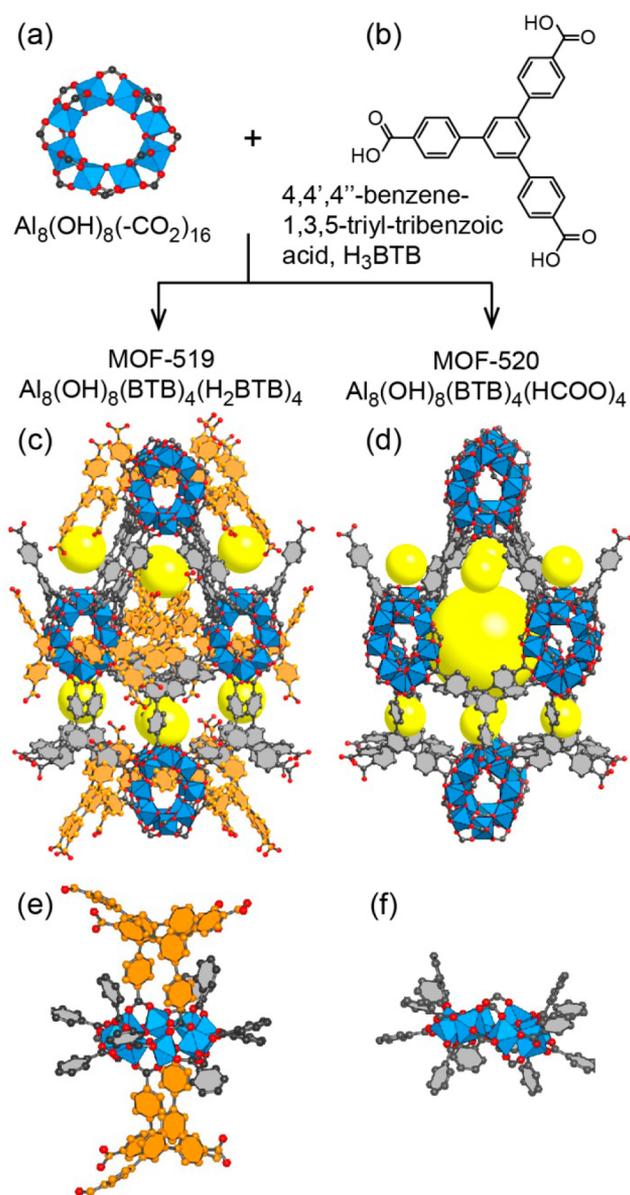
**Figure 1.** MOF-519 and MOF-520 are built from octametallic inorganic SBUs (a) and the organic BTB linker (b). In MOF-519 (c), part of the framework void space is occupied by dangling BTB ligands, which are represented in orange (the framework linkers are represented in gray). There are four of these ligands in each SBU (e). In MOF-520 (d), formate ligands replace the extra BTB ligands in the SBU (f), resulting larger pores.

was used to determine the crystal structure of this new MOF (Supporting Information, SI, section S1). The material crystallizes in the tetragonal space group $P4_22_12$.[13] The inorganic secondary building unit (SBU) of MOF-519 consists of eight octahedrally coordinated aluminum atoms that are cornered joined by doubly bridging OH groups (Figure 1a). Arrangements with vertex-sharing octahedral atoms are known in other aluminum MOFs but with rod-shaped metal oxide SBUs.[14] In MOF-519 the discrete, octametallic, ring-shaped SBU motif is known with several other elements as discrete structures,[15] and it is also present in the aluminum MOF CAU-1,[16] where 12 carboxylates and 8 methoxy ligands are holding together the 8 aluminum atoms. In contrast MOF-519 has 12 carboxylate BTB links (colored gray in Figure 1) used to build

the extended structure and 4 terminal BTB ligands (colored orange in Figure 1). The latter are linked only by one of their carboxylates to the SBU, with the remaining two carboxylates protruding into the interior of the three-dimensional structure of this MOF. The overall framework topology of MOF-519 is a (12,3)-connected net, which can be simplified to the topological type **sum**,[17] previously observed in a beryllium-BTB MOF.[18] In MOF-519 sinusoidal channels are formed and are connected by windows of maximum diameter of 7.6 Å, as determined by PLATON.[19]

Crystals of MOF-520 were prepared under different synthetic conditions,[20] replacing nitric acid by formic acid. MOF-520 has a crystal structure that is closely related to that of MOF-519. It crystallizes in the same space group and with similar lattice parameters.[21] It is composed of the same octametallic SBU, and it has the same overall framework topology, but instead of four terminal BTB ligands, it has four formate ligands. This allows for a larger void space in MOF-520 (16.2 × 9.9 Å) (Figure 1d) compared to MOF-519.

Prior to the methane adsorption measurements, we recorded the $N_2$ isotherms of MOF-519 and MOF-520 at 77 K to confirm the presence of the permanent microporosity. Both MOFs showed steep $N_2$ uptake below $P/P_0 = 0.05$, and the uptake values were nearly saturated around $P/P_0 = 0.2$ (Figure S5). $N_2$ molecules were desorbed when the pressure was reduced, which clearly indicates that these MOFs have permanent microporosity. The $N_2$ uptake by MOF-520 is greater than the one by MOF-519 because of the absence of protruded BTB ligands in the pore so that MOF-520 shows larger pore volume (0.94 and 1.28 $cm^3$ $g^{-1}$ for MOF-519 and MOF-520, respectively). The BET (Langmuir) surface areas of MOF-519 and MOF-520 are estimated to be 2400 (2660) $m^2$ $g^{-1}$ and 3290 (3630) $m^2$ $g^{-1}$, respectively.

Methane adsorption isotherms for MOF-519 and MOF-520 were measured at 298 K using a high-pressure volumetric gas adsorption analyzer. The excess methane isotherms for MOF-519 and MOF-520 are shown in Figures S10−S12. Initially the methane uptake increases with an increase in the pressure, while the uptake saturates at around 80 bar (215 and 288 $cm^3$ $g^{-1}$ for MOF-519 and MOF-520, respectively). In terms of the gravimetric uptake capacity, MOF-520 outperforms MOF-519 up to 80 bar, which is not surprising because of the larger surface area and pore volume of MOF-520. Considering the practical application of methane storage, the total volumetric methane uptake is rather relevant. Therefore, we estimated the total volumetric methane uptake using the crystal density of MOFs and the following equation: total uptake = excess uptake + (bulk density of methane) × (pore volume).

As shown in Figure 2, MOF-519 shows high total volumetric methane uptake capacity. Considering that MOF-519 does not have strong binding sites (e.g., open metal sites),[22] it is likely that the average pore diameter of MOF-519 is of optimal size to confine methane molecules in the pore. In Table 1 we compare the total uptake and the working capacity of MOF-519 and MOF-520 with the materials that have been recently identified as the best methane adsorbents. At 35 bar, the total uptake capacity of MOF-519 (200 $cm^3$ $cm^{-3}$) is approaching that of Ni-MOF-74 (230 $cm^3$ $cm^{-3}$). At 80 bar MOF-519 outperforms any other reported MOF, with a total volumetric capacity of 279 $cm^3$ $cm^{-3}$.

Since MOF-519 shows high total volumetric uptake capacity, we also evaluated whether this material can exceed the energy density of compressed natural gas (CNG) at 250 bar (which is

**Table 1. Total Methane Uptake and Working Capacity (Desorption at 5 bar) at 35, 80, and 250 bar and 298 K**

| material | surface area, $m^2 g^{-1}$ | | $V_p$, $cm^3 g^{-1}$ | density, $g\ cm^{-3}$ | total uptake at 35 bar, $cm^3\ cm^{-3}$ | total uptake at 80 bar, $cm^3\ cm^{-3}$ | total uptake at 250 bar,[a] $cm^3\ cm^{-3}$ | working capacity at 35 bar, $cm^3\ cm^{-3}$ | working capacity at 80 bar, $cm^3\ cm^{-3}$ | working capacity at 250 bar, $cm^3\ cm^{-3}$ |
|---|---|---|---|---|---|---|---|---|---|---|
| | BET | Langmuir | | | | | | | | |
| MOF-519 | 2400 | 2660 | 0.938 | 0.953 | 200 | **279** | 355 | 151 | **230** | 306 |
| MOF-520 | 3290 | 3930 | 1.277 | 0.586 | 162 | 231 | 302 | 125 | 194 | 265 |
| MOF-5[b] | 3320 | 4400 | 1.38 | 0.605 | 126 | 198 | 328 | 104 | 176 | 306 |
| MOF-177[b] | 4500 | 5340 | 1.89 | 0.427 | 122 | 205 | 350 | 102 | 185 | 330 |
| MOF-205[b] | 4460 | 6170 | 2.16 | 0.38 | 120 | 205 | 345 | 101 | 186 | 326 |
| MOF-210[b] | 6240 | 10400 | 3.6 | 0.25 | 82 | 166 | **377** | 70 | 154 | **365** |
| Ni-MOF-74[c] | | 1438 | 0.51 | 1.195 | **230** | 267 | – | 115 | 152 | – |
| HKUST-1[c] | | 1977 | 0.69 | 0.881 | 225 | 272 | – | **153** | 200 | – |
| PCN-14[c] | | 2360 | 0.83 | 0.819 | 200 | 250 | – | 128 | 178 | – |
| AX-21[c] | | 4880 | 1.64 | 0.487 | 153 | 222 | – | 103 | 172 | – |
| bulk $CH_4$ | N/A | N/A | N/A | N/A | 33 | 83 | 263 | 29 | 79 | 260 |

[a]Calculated with a dual site Langmuir model. [b]Data from ref 9. [c]Data from ref 6a.
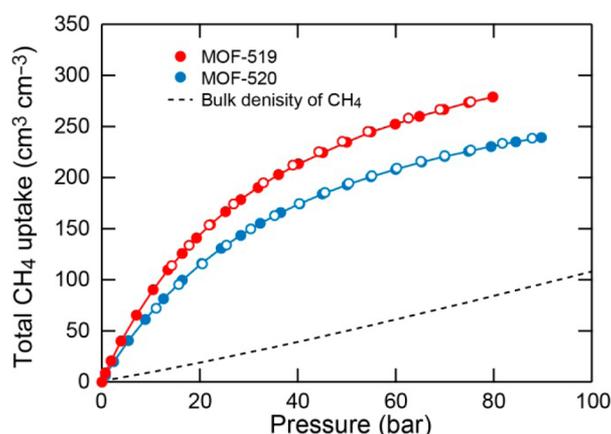


**Figure 2.** MOF-519 and MOF-520 show high total methane volumetric uptake. For comparison, bulk density of methane is represented as broken curve. Filled markers represent adsorption points, and empty markers represent desorption points.



**Figure 3.** Comparison of the working capacity for MOF-519, MOF-520, the top performing MOFs, and the porous carbon AX-21. Values are calculated as the difference between the uptake at 35 bar (blue) or 80 bar (orange) and the uptake at 5 bar. As a reference, the working capacity for bulk methane data are overlaid. Data for MOF-177, MOF-5, MOF-205, and MOF-210 were obtained from ref 9, and data for HKUST-1, PCN-24, Ni-MOF-74, and AX-21 were obtained from ref 6a.

a pressure value used for some natural gas fueled automobiles). Here, the total volumetric uptake of MOF-519 and MOF-520 was calculated by extrapolation of the total uptake isotherm using a dual site Langmuir model (Figures S13 and S14) and found to be 355 $cm^3\ cm^{-3}$, far exceeding CNG (263 $cm^3\ cm^{-3}$).

The same model was used to calculate the uptake for other methane adsorbents (Figures S15−S18), and with this fitting data, the working capacity of methane (desorption pressure is at 5 bar) was obtained (Table 1 and Figure 3). The working capacity of MOF-519 at 35 bar is 151 $cm^3\ cm^{-3}$, while at 80 bar this MOF is able to deliver 230 $cm^3\ cm^{-3}$, which is the largest obtained for any of the top performing MOFs and porous carbon AX-21. At 80 bar, a tank filled with MOF-519 would deliver almost three times more methane than an empty tank.

## ■ ASSOCIATED CONTENT

### Ⓢ Supporting Information

Detailed synthetic procedures and characterization, powder X-ray diffraction patterns, thermogravimetric analysis trace, low pressure methane adsorption analysis, high pressure methane adsorption details and crystallographic data (CIF files), and complete ref 9. This material is available free of charge via the Internet at http://pubs.acs.org.

## ■ AUTHOR INFORMATION

### Corresponding Author
yaghi@berkeley.edu

### Notes
The authors declare no competing financial interest.

## ■ ACKNOWLEDGMENTS

## ■ REFERENCES

(1) Methane Opportunities for Vehicular Energy, Advanced Research Project Agency − Energy, U.S. Dept. of Energy, Funding Opportunity No. DE-FOA-0000672, 2012. https://arpa-e-foa.energy.gov/Default.aspx?Search=DE-FOA-0000672 (accessed on March 17, 2014).

(2) (a) Furukawa, H.; Cordova, K. E.; O'Keeffe, M.; Yaghi, O. M. *Science* **2013**, *341*, 974. *Science* **2013**, *341*, 1230444. (b) Cook, T. R.; Zheng, Y.-R.; Stang, P. J. *Chem. Rev.* **2013**, *113*, 734. (c) McKinlay, A. C.; Morris, R. E.; Horcajada, P.; Ferey, G.; Gref, R.; Couvreur, P.; Serre, C. *Angew. Chem., Int. Ed.* **2010**, *49*, 6260. (d) Mueller, U.; Schubert, M.; Teich, F.; Puetter, H.; Schierle-Arndt, K.; Pastre, J. *J. Mater. Chem.* **2006**, *16*, 626. (e) Shimizu, G. K. H.; Vaidhyanathan, R.; Taylor, J. M. *Chem. Soc. Rev.* **2009**, *38*, 1430. (f) Corma, A.; Garcia, H.; Llabres i Xamena, F. X. *Chem. Rev.* **2010**, *110*, 4606. (g) Meek, S. T.; Greathouse, J. A.; Allendorf, M. D. *Adv. Mater.* **2011**, *23*, 249. (h) Kitagawa, S.; Kitaura, R.; Noro, S. *Angew. Chem., Int. Ed.* **2004**, *43*, 2334.

(3) (a) Murray, L. J; Dincă, M.; Long, J. R. *Chem. Soc. Rev.* **2009**, *38*, 1294. (b) Suh, M.; Park, H.; Prasad, T.; Lim, D. *Chem. Rev.* **2012**, *112*, 782. (c) Caskey, S. R.; Wong-Foy, A. G.; Matzger, A. J. *J. Am. Chem. Soc.* **2008**, *130*, 10870. (d) Lin, X.; Jia, J.; Zhao, X.; Thomas, K. M.; Blake, A. J.; Walker, G. S.; Champness, N. R.; Hubberstey, P.; Schroeder, M. *Angew. Chem., Int. Ed.* **2006**, *45*, 7358. (e) Yang, S.; Lin, X.; Lewis, W.; Suyetin, M.; Bichoutskaia, E.; Parker, J. E.; Tang, C. C.; Allan, D. R.; Rizkallah, P. J.; Hubberstey, P.; Champness, N. R.; Thomas, K. M.; Blake, A. J.; Schröeder, M. *Nat. Mater.* **2012**, *11*, 710. (f) Xiang, S.; He, Y.; Zhang, Z.; Wu, H.; Zhou, W.; Krishna, R.; Chen, B. *Nat. Commun.* **2012**, *3*, 956. (g) Li, T.; Chen, D.-L.; Sullivan, J. E.; Kozlowski, M. T.; Johnson, J. K.; Rosi, N. L. *Chem. Sci.* **2013**, *4*, 1746.

(4) (a) Noro, S.; Kitagawa, S.; Kondo, M.; Seki, K. *Angew. Chem., Int. Ed.* **2000**, *39*, 2082. (b) Eddaoudi, M.; Kim, J.; Rosi, N.; Vodak, D.; Wachter, J.; O'Keeffe, M.; Yaghi, O. M. *Science* **2002**, *295*, 469. (c) Makal, T.; Li, J.; Lu, W.; Zhou, H. *Chem. Soc. Rev.* **2012**, *41*, 7761. (d) Konstas, K.; Osl, T.; Yang, Y.; Batten, M.; Burke, N.; Hill, A. J.; Hill, M. R. *J. Mater. Chem.* **2012**, *22*, 16698. (e) Stoeck, U.; Krause, S.; Bon, V.; Senkovska, I.; Kaskel, S. *Chem. Commun.* **2012**, *48*, 10841.

(5) Chui, S. S.-Y.; Lo, S. M.-F.; Charmant, J. P. H.; Orpen, A. G.; Williams, I. D. *Science* **1999**, *283*, 1148.

(6) (a) Mason, J. A.; Veenstra, M.; Long, J. R. *Chem. Sci.* **2014**, *5*, 32. (b) Peng, Y.; Krungleviciute, V.; Eryazici, I.; Hupp, J. T.; Farha, O. K.; Yildirim, T. *J. Am. Chem. Soc.* **2013**, *135*, 11887.

(7) (a) Rosi, N. L.; Kim, J.; Eddaoudi, M.; Chen, B. L.; O'Keeffe, M.; Yaghi, O. M. *J. Am. Chem. Soc.* **2005**, *127*, 1504. (b) Dietzel, P. D. C.; Panella, B.; Hirscher, M.; Blom, R.; Fjellvåg, H. *Chem. Commun.* **2006**, 959.

(8) Li, H.; Eddaoudi, M.; O'Keeffe, M.; Yaghi, O. M. *Nature* **1999**, *402*, 276.

(9) Furukawa, H.; et al. *Science* **2010**, *329*, 424.

(10) Chae, H. K.; Siberio-Perez, D. Y.; Kim, J.; Go, Y.-B.; Eddaoudi, M.; Matzger, A. J.; O'Keeffe, M.; Yaghi, O. M. *Nature* **2004**, *427*, 523.

(11) Ma, S.; Sun, D.; Simmons, J. M.; Collier, C. D.; Yuan, D.; Zhou, H.-C. *J. Am. Chem. Soc.* **2008**, *130*, 1012.

(12) In a Teflon vessel, 109 mg of H$_3$BTB were dissolved in 9 mL of DMF. A 0.2 M solution of aluminum nitrate (0.675 mL) and nitric acid (0.675 mL) were subsequently added to the solution. The vessel was placed in a stainless steel autoclave and heated at 150 °C for 72 h,

after which time it was cooled to room temperature. A white microcrystalline powder was recovered by centrifugation and washed three times with 10 mL of anhydrous DMF.

(13) Crystallographic data for C$_{216}$H$_{60}$Al$_8$O$_{56}$, MOF-519: $M_w$ = 3766.48 g mol$^{-1}$, tetragonal, space group: $P4_22_12$, $a$ = 19.289(1) Å, $c$ = 36.030(1) Å, $V$ = 13393.0(1) Å$^3$, $D_{calcd}$ = 0.934 g cm$^{-3}$, $\lambda$ = 0.8903 Å, $Z$ = 4, $R_1$ = 0.1112, $wR_2$ = 0.2794, GOF = 1.058.

(14) (a) Loiseau, T.; Serre, C.; Huguenard, C.; Fink, G.; Taulelle, F.; Henry, M.; Bataile, T.; Férey, G. *Chem.—Eur. J.* **2004**, *10*, 1373. (b) Bloch, E. D.; Britt, D. K.; Doonan, C. J.; Uribe-Romo, F. J.; Furukawa, H.; Long, J. R.; Yaghi, O. M. *J. Am. Chem. Soc.* **2010**, *132*, 14382.

(15) (a) Cador, O.; Gatteschi, D.; Sessoli, R.; Larsen, F. K.; Overgaard, J.; Barra, A.-L.; Teat, S. J.; Timco, G. A.; Winpenny, R. E. P. *Angew. Chem., Int. Ed.* **2004**, *43*, 5196. (b) van Slageren, J.; Sessoli, R.; Gatteschi, D.; Smith, A. A.; Helliwell, M.; Winpenny, R. E. P.; Cornia, A.; Barra, A.-L.; Jansen, A. G. M.; Rentschler, E.; Timco, G. A. *Chem.—Eur. J.* **2002**, *8*, 277.

(16) Ahnfeldt, T.; Guillou, N.; Gunzelmann, D.; Margiolaki, I.; Loiseau, T.; Ferey, G.; Senker, J.; Stock, N. *Angew. Chem., Int. Ed.* **2009**, *48*, 5163.

(17) O'Keeffe, M.; Yaghi, O. M. *Chem. Rev.* **2012**, *112*, 675.

(18) Sumida, K.; Hill, M.; Horike, S.; Dailly, A.; Long, J. *J. Am. Chem. Soc.* **2009**, *131*, 15120.

(19) Spek, A. L. *Acta Crystallogr.* **2009**, *D65*, 148.

(20) In a 20 mL scintillation vial, 90 mg of Al(NO$_3$)$_3$·9H$_2$O and 75 mg of H$_3$BTB were dissolved in 14 mL of DMF. Formic acid (1.4 mL) was subsequently added to the solution. The vial was placed in an oven preheated at 130 °C for 48 h, yielding white prismatic crystals of MOF-520.

(21) Crystallographic data for C$_{115}$H$_{76}$Al$_8$O$_{41}$, MOF-520: $M_w$ = 2328.59 g mol$^{-1}$, tetragonal, space group: $P4_22_12$, $a$ = 18.878(4) Å, $c$ = 37.043(8) Å, $V$ = 13202(6) Å$^3$, $D_{calcd}$ = 0.586 g cm$^{-3}$, $\lambda$ = 0.95403 Å, $Z$ = 4, $R_1$ = 0.0874, $wR2$ = 0.2522, GOF = 1.166.

(22) From the low-pressure methane isotherm data, we estimated isosteric heats of adsorption ($Q_{st}$) of methane in MOF-519 and MOF-520. The initial $Q_{st}$ values for MOF-519 and MOF-520 are 14.6 and 13.6 kJ mol$^{-1}$, respectively. These values are smaller than MOFs with open metal sites; Ni-MOF-74 and HKUST-1 (21.4 and 17.0 kJ mol$^{-1}$).[6b]